symmetry

MDPI

Article

The Inhomogeneous Road to Chiral Symmetry Breaking: A Ginzburg–Landau–Langevin Analysis

Theo F. Motta and Gastão Krein *

Instituto de Física Teórica, Universidade Estadual Paulista, São Paulo 01140-070, SP, Brazil; theo.motta@unesp.br
* Correspondence: gastao.krein@unesp.br

Abstract: We investigate the time evolution of the quark condensate toward a chiral symmetry broken phase in hot and dense quark matter using a field-theoretic quark model with nonlocal chiral-invariant four-fermion coupling. By purposely selecting a parameter set in which inhomogeneous phases are energetically disfavored, we nonetheless observe the emergence of metastable patterned configurations that appear to persist for remarkably long timescales. These findings suggest that even when not fully stable, inhomogeneous phases may play a significant role in the dynamics of chiral symmetry breaking and restoration. To gain deeper insight into these phenomena, we also analyze the impact of the dimensionality of coordinate space on both the formation and stability of inhomogeneous chiral condensates.

Keywords: quantum chromodynamics; chiral symmetry; quark matter; QCD phase diagram; inhomogeneous phases

1. Introduction

There are many open questions when it comes to inhomogeneous chiral symmetry breaking. Since inhomogeneous nuclear matter phases were first proposed over 80 years ago [1], it remains unclear whether or not such phases are present in QCD. However, many interesting developments have been achieved recently, and evidence has been building that some type of phase where chiral symmetry is inhomogeneously broken might be realized [2–4]. Nevertheless, it is a rather subtle point with many facets. For instance, most of the evidence for this phenomenon comes from QCD-inspired models such as the Gross–Neveu model [5–8], the Nambu–Jona–Lasinio (NJL) model [9,10], and the quark–meson model [11–13]. However, such low-energy models come with costs for their simplicity and calculability. For example, although there is very solid evidence for inhomogeneous phases in the 1+1 dimensional Gross–Neveu model [5,14], it is still unclear what happens in larger-dimensional spaces. References [15–18], to name a few, find that in larger-dimensional spaces, these phases might vanish or, at least, be strongly modified. Furthermore, as the number of dimensions increases, unrenormalizable models—such as the Gross–Neveu and Nambu–Jona–Lasinio (NJL)—must be defined together with some regularization scheme and scale. Perhaps unsurprisingly, strong dependence of the inhomogeneous phases on the regularization is found [19–22]. On top of these difficulties comes the fact that a majority of works that search for evidence of inhomogeneous phases are conducted in mean-field approximation. Including quantum and thermal fluctuations might disorder spatially nontrivial condensates completely [23] or perhaps change the nature of their transition to and from the restored phase [24].

check for updates

Academic Editor: Charalampos Moustakidis

Received: 13 March 2025
Revised: 1 April 2025
Accepted: 6 April 2025
Published: 9 April 2025

Citation: Motta, T.F.; Krein, G. The Inhomogeneous Road to Chiral Symmetry Breaking: A Ginzburg–Landau–Langevin Analysis. *Symmetry* **2025**, *17*, 568. https://doi.org/10.3390/sym17040568

Copyright: © 2025 by the authors. Licensee MDPI, Basel, Switzerland. This article is an open access article distributed under the terms and conditions of the Creative Commons Attribution (CC BY) license (https://creativecommons.org/licenses/by/4.0/).

One might wonder, however, if these phases happen to be unstable, could they still be metastable? Could it be that, although they would eventually decay to a homogeneous phase, they happen to live long enough to leave some experimental signature? In this work, we explore this possibility using a Ginzburg–Landau–Langevin (GLL) field equation for the quark condensate time evolution. GLL field equations are widely used in field theory treatments of dynamical phase transitions [25,26]. Taking a field-theoretic quark model that predicts that inhomogeneous phases are *not* stable [27,28], we calculate under a temperature quench scenario what would happen with a restored phase once it cools down into the broken phase. In a quench scenario, the temperature of the system changes suddenly; a classic example is a temperature quench in a spin system, where a sudden drop in temperature drives the system irreversibly from a spin-disordered phase into a spin-ordered phase. Such an approach was used previously in previous studies [29,30], with the same model we consider here, but neglecting fluctuations; that is, the Langevin part of the GLL equation was neglected, and the resulting equation is the celebrated time-dependent Ginzburg–Landau equation. Moreover, in these studies, the number of spatial dimensions in the meson GGL dynamics was restricted to one spatial dimension. This is because, models in spaces with more than one dimension still find that the most stable configurations are 1d structures embedded in the larger dimensional space (see e.g., Ref. [15]). In this paper, we take two significant steps forward, taking into account the fluctuations and performing GGL simulations in one, two, and three spatial dimensions. Other studies closely related to ours using GLL equations to study the dynamics of quark condensate can be found in Refs. [31–33].

In the next section, we briefly review some of the basic facts about inhomogeneous phases. Then, we introduce the model and discuss some archetypical examples of the condensate's evolution. We argue that it might indeed live for very long periods of time, enough to leave experimental signatures.

2. Inhomogeneous Phases

The simplest of the QCD-inspired models is, without a doubt, the Gross–Neveu model. As usual, however, simple fundamental interactions give rise to complex and nontrivial phenomena, especially in many-body systems. The model, defined by the Euclidean action in 1 + 1 dimensional space–time

$$S_E = -\int d^2x \left(\sum_{i=1}^{N} \bar{\psi}_i \left(i\gamma^\mu \partial_\mu - m_0 \right) \psi_i + \frac{1}{2} g^2 \left(\sum_{i=1}^{N} \bar{\psi}_i \psi_i \right)^2 \right) \tag{1}$$

describes N (color times flavor) equal-mass fermions interacting via a scalar contact interaction. In the case of zero bare fermion masses $m_0 = 0$, it manifests a discrete chiral symmetry, which is broken in the vacuum. Even away from the chiral limit, however, the model can be solved analytically (in the large N limit) and for moderate chemical potential and low temperatures, a spatially inhomogeneous solution appears. The effective fermion mass in this phase can be parametrized by the Jacobi elliptic functions sn, cn, and dn

$$M_{1\mathrm{D}}(x) = \Delta\nu \frac{\mathrm{sn}(\Delta x \mid \nu)\, \mathrm{cn}(\Delta x \mid \nu)}{\mathrm{dn}(\Delta x \mid \nu)}. \tag{2}$$

For an elliptic modulus of $\nu = 1$, this would give rise to a hyperbolic tangent shape

$$M_{1\mathrm{D}}(x) \xrightarrow{\nu \to 1} \Delta \tanh \Delta x, \tag{3}$$

and as the modulus goes to zero, this becomes a $\sin(\Delta x)$ function. This type of phase, known as a real-kink-crystal (RKC), is energetically favored over homogeneous phases over a significant portion of the Gross–Neveu model. Although more complicated, this can also be investigated in the NJL model. If one postulates the existence of an inhomogeneous condensate and calculates the free energy, one sees that an RKC is also more favorable in NJL for low temperatures and moderate chemical potentials [13].

Less relevant to this study, but still most relevant to the field, are other types of spatial patterned phases such as the chiral spiral, chiral density waves, twisted kink crystals, and so on [34–40]. They are found abundantly in models of strong interactions and might be realized in QCD. For this study, we chose to use a nonlocal version of the NJL model, in which the fermion fields interact through a nonlocal chiral invariant four-fermion coupling. This bypasses the renormalization and regularization issues, since a form factor modeling the nonlocal four-fermion coupling makes all loop integrals finite and, also, might better correspond to a QCD-like interaction where the quark–quark potential is also nonlocal.

3. The Model

Following the approach in Refs. [27–30], we take a nonlocal NJL model, where the contact interaction between the quarks contains a form-factor. Its Euclidean action, in 3 + 1 dimensions, can be written as

$$S_E = \int d^4x \left[-i\bar{\psi}(x)\partial\!\!\!/\psi(x) - \frac{G}{2} j_a(x) j_a(x) \right], \tag{4}$$

where the current j_a is

$$j_a(x) = \int d^4x' \mathcal{G}(x') \bar{\psi}\left(x + \frac{x'}{2}\right) \Gamma_a \psi\left(x - \frac{x'}{2}\right), \tag{5}$$

and where the form-factor $\mathcal{G}(x)$, or $g(p)$ in momentum space, is chosen to be Gaussian-shaped:

$$g(p) = e^{-p^2/\Lambda^2}. \tag{6}$$

Note that this acts as a regulator. We can then choose parameters where the inhomogeneous phase is not fully stable in mean-field. With

$$G = 14.668\ \text{GeV}^{-2}, \quad \text{and} \quad \Lambda = 1.046\ \text{GeV}, \tag{7}$$

this is the case, and we obtain a reasonable chiral-limit pion decay constant of $f_\pi = 86$ MeV and a vacuum quark condensate of $\langle\bar{\psi}\psi\rangle = -(270\ \text{MeV})^3$ [41,42]. Equation (4) describes a system where the quarks interact via a contact current–current interaction; however, the currents contain a non-local form-factor (see e.g., Ref. [43]). This non-locality is meant to model gluonic effects as suggested by the instanton picture of the QCD vacuum [44,45]. We can then employ a Ginzburg–Landau analysis; that is, we perform an expansion of the bosonized effective action in powers of the condensates and their spatial gradients (see Ref. [27] for details):

$$\Omega_{GL}[\phi^a] = \int d^4x\, \omega(T, \mu, \phi^a(\vec{x})), \tag{8}$$

where the free-energy density

$$\begin{aligned} \omega(T, \mu, \phi^a(\vec{x})) = &\frac{\alpha_2}{2}\phi^2 + \frac{\alpha_4}{4}\left(\phi^2\right)^2 + \frac{\alpha_{4b}}{4}(\nabla\phi)^2 + \frac{\alpha_6}{6}\left(\phi^2\right)^3 + \frac{\alpha_{6b}}{6}(\phi, \nabla\phi)^2 \\ &+ \frac{\alpha_{6c}}{6}\left[\phi^2(\nabla\phi)^2 - (\phi, \nabla\phi)^2\right] + \frac{\alpha_{6d}}{6}(\Delta\phi)^2, \end{aligned} \tag{9}$$

where the coefficients α are obtained via an expansion of the full effective action with respect to the size of the condensates and their spatial derivatives

$$\begin{aligned}
\alpha_2 &= \frac{1}{G} - 8N_c \oint\!\!\!\!\!\!\int \frac{g^2}{p_n^2}, \\
\alpha_4 &= 8N_c \oint\!\!\!\!\!\!\int \frac{g^4}{p_n^4}, \\
\alpha_6 &= -8N_c \oint\!\!\!\!\!\!\int \frac{g^6}{p_n^6}, \\
\alpha_{4b} &= 8N_c \oint\!\!\!\!\!\!\int \frac{g^2}{p_n^4}\left(1 - \frac{2}{3}\frac{g'}{g}\vec{p}^2\right), \\
\alpha_{6b} &= -40N_c \oint\!\!\!\!\!\!\int \frac{g^4}{p_n^6}\left(1 - \frac{26}{15}\frac{g'}{g}\vec{p}^2 + \frac{8}{5}\frac{g^2}{g^2}\vec{p}^2 p_n^2\right), \\
\alpha_{6c} &= -24N_c \oint\!\!\!\!\!\!\int \frac{g^4}{p_n^6}\left(1 - \frac{2}{3}\frac{g'}{g}\vec{p}^2\right), \\
\alpha_{6d} &= -4N_c \oint\!\!\!\!\!\!\int \frac{g^2}{p_n^6}\left[1 - \frac{2}{3}\frac{g'}{g}\vec{p}^2 + \frac{1}{5}\left(\frac{g'^2}{g^2} + \frac{g''}{g}\right)\vec{p}^4\right],
\end{aligned} \tag{10}$$

where $\oint\!\!\!\!\!\!\int$ is the Matsubara sum together with momentum integration

$$\oint\!\!\!\!\!\!\int = T\sum_{\omega_n}\int d^3p. \tag{11}$$

The time evolution of the bosonized fields according to the Ginzburg–Landau–Langevin (GLL) framework [25,26] is given by

$$\eta\frac{\partial\phi^a(\vec{x},t)}{\partial t} = -\frac{\delta\Omega_{GL}}{\delta\phi^a(\vec{x},t)} + \xi(\vec{x},t), \tag{12}$$

where ξ is a noise field representing quantum and thermal fluctuations, and η is the dissipation coefficient. This is approach is phenomenological. It describes a dissipative stochastic process compatible with the dissipation–fluctuation relations, which relate η and ξ. They can be formally obtained from the microscopic theory via the influence functional formalism [46]. The role of η is to drive the initial out-of-equilibrium state to an equilibrium state. It is a transport coefficient that dictates how fast the system approaches equilibrium. The physics behind η in this kind of model are the $\sigma \leftrightarrow \bar{q}q$ and $\sigma \leftrightarrow \pi\pi$ dissipative processes. Equation (12) is an approximation to a GLL equation that also includes a second-order time derivative [32], an approximation that is valid to a close to equilibrium situation. For us here, it is less important to obtain a precise calculation of the dissipation coefficient in this specific model and more important to try and understand how they influence the dynamic evolution of the system. We therefore perform our calculation with some ballpark values for η and the corresponding leading order term for ξ in a high-temperature expansion [31,32], namely:

$$\langle\xi(\vec{x},t)\xi(\vec{x}',t')\rangle = 2\eta T\delta(t-t')\delta^{(3)}(x-x'). \tag{13}$$

Note that, by rescaling the time variable as $\tau = t/\eta$, we are able to avoid having to numerically define η. We shall do this for the rest of this paper; however, we will expand on this in the Discussion section.

To further simplify the problem, we shall evolve only the scalar condensate, i.e., where $\phi = (\sigma, \vec{\pi})$, and leave the pion fields frozen. Since the pion fields should always go to zero at the end of the evolution, this approximation can be thought of as a rapidly

dissipating pion field. We reserve for a future study to take into account the pion fields in a GLL framework [31].

Figure 1 shows the phase diagram of the model with the chosen parameter set. Note that the dotted black line, which shows the stability boundary of the restored solution with respect to inhomogeneous patterning, is deep inside the broken phase. Furthermore, all calculations will assume the system evolves along the gray arrow, suddenly (quenched scenario), from the restored phase to the broken phase. This point optimizes the validity region of the Ginzburg–Landau analysis, since the order parameter vanishes close to the tri-critical point, and the spatial gradients vanish close to the proto-Lifschitz (A proto-Lifschitz point is defined in Ref. [2], and it refers to the point where the stability boundary of the symmetric phase against inhomogeneous perturbation meets the spinodal *to the left of* the homogeneous first-order transition.) point—and the GL analysis is precisely an expansion of the powers of the condensate and its gradients—at this point, the GL action should well reproduce the full effective action of the theory. The right-hand side plot in Figure 1 shows the free energy as a function of the σ field at this point.

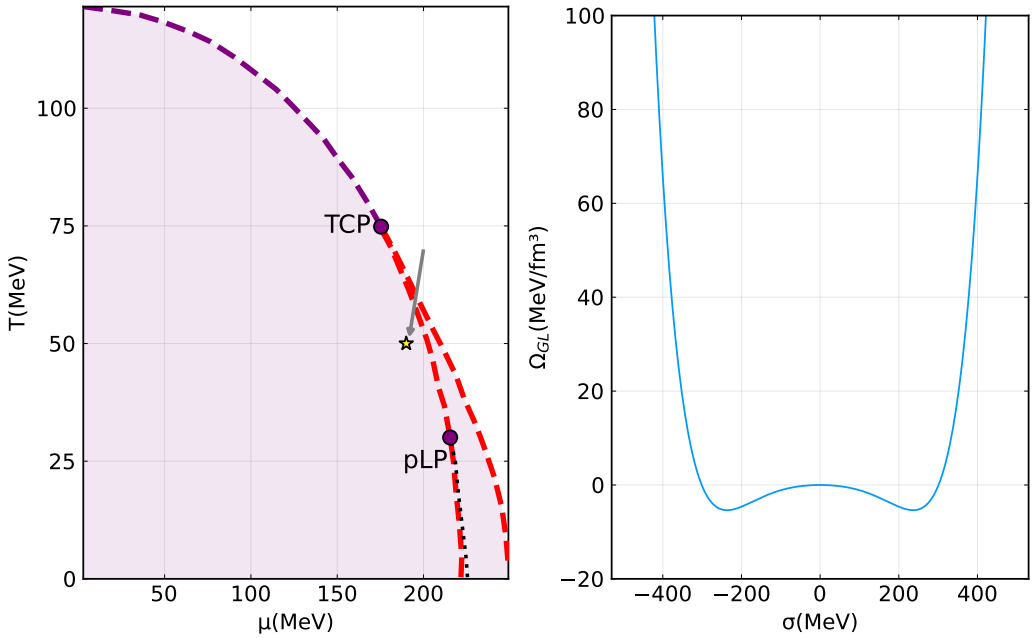


Figure 1. The plot on the left shows the phase diagram in the model with the parameter choice $G = 14.668\ \text{GeV}^{-2}$ and $\Lambda = 1.046$ GeV. The tri-critical point (TCP) and proto-Lifschitz point (pLP) are shown as dots. The purple line is the homogeneous chiral second order transition, the two red lines are the spinodals, and the black dotted line marks the boundary of stability of the restored solution with respect to inhomogeneous perturbations. The yellow star is the point where the calculations in this paper take place, and the gray arrow represents symbolically the path the system takes from the restored phase to the broken phase. The plot on the right shows the Ginzburg–Landau potential calculated at the yellow star point shown on the left plot, for which (μ,T) = (190 MeV, 50 MeV). In essence, the purple region of the figure on the left shows when the effective potential, such as the plot on the right, has minima such that $\sigma \neq 0$. On the purple dashed line, the potential is effectively flat, and between the two red lines there are minima both on $\sigma = 0$ and $\sigma \neq 0$.

4. Archetypes of the Condensate's Evolution

The evolution of Equation (12) requires an initial condition and spatial boundary conditions. Our main goal here is to model a heavy-ion collision scenario where the system is quenched from a high-temperature state to a low-temperature and large quark chemical potential phase. Such cold and dense states of matter will be explored by experiments planned at NICA [47], FAIR [48] and J-PARC [49] . Therefore, we take the quenched scenario

where the broken $\sigma = 0$ phase is suddenly put back into a broken phase, in particular, close to the tri-critical point and the proto-Lifschitz point. Since one of the points of the paper is to consider fluctuations, the initial condition is simply taken to be

$$\sigma(\vec{x}, \tau \to 0) = \xi(\vec{x}, 0). \tag{14}$$

As for the spatial part, we choose to use free boundary conditions, i.e., the system is free to settle its edges at any minima of the potential. Let us now explore what happens with the evolution of the system as we progressively increase the number of spatial dimensions.

4.1. 1 + 1 Dimensions

In one single spatial dimension, some work has already been conducted in the absence of fluctuations [29,30].

In Figure 2, we see some archetypic evolutions of the condensate for T = 50 MeV and $\mu = 190$ MeV. For τ_1, which is the initial condition, the system is initialized as fluctuating around zero. The gray lines show some intermediary steps, and $\tau_2, \tau_3, \ldots \tau_5$ show snapshots of the evolution 3000 steps of $\Delta\tau = 10^{-4}\eta^{-1}$ apart. The system might move directly towards the positive or negative minimum of the potential (around $\sigma = \pm 240$ MeV) or potentially create inhomogeneous configurations. Once those are formed, they will eventually collapse to a homogeneous configuration around one of the minima; however, these patterned phases last for very long times, in some cases, longer than the longest run of our numerical evolution of Equation (12). Nevertheless, it is only when we disregard the noise terms ξ that they will last for arbitrarily long. Otherwise, all of them eventually decay.

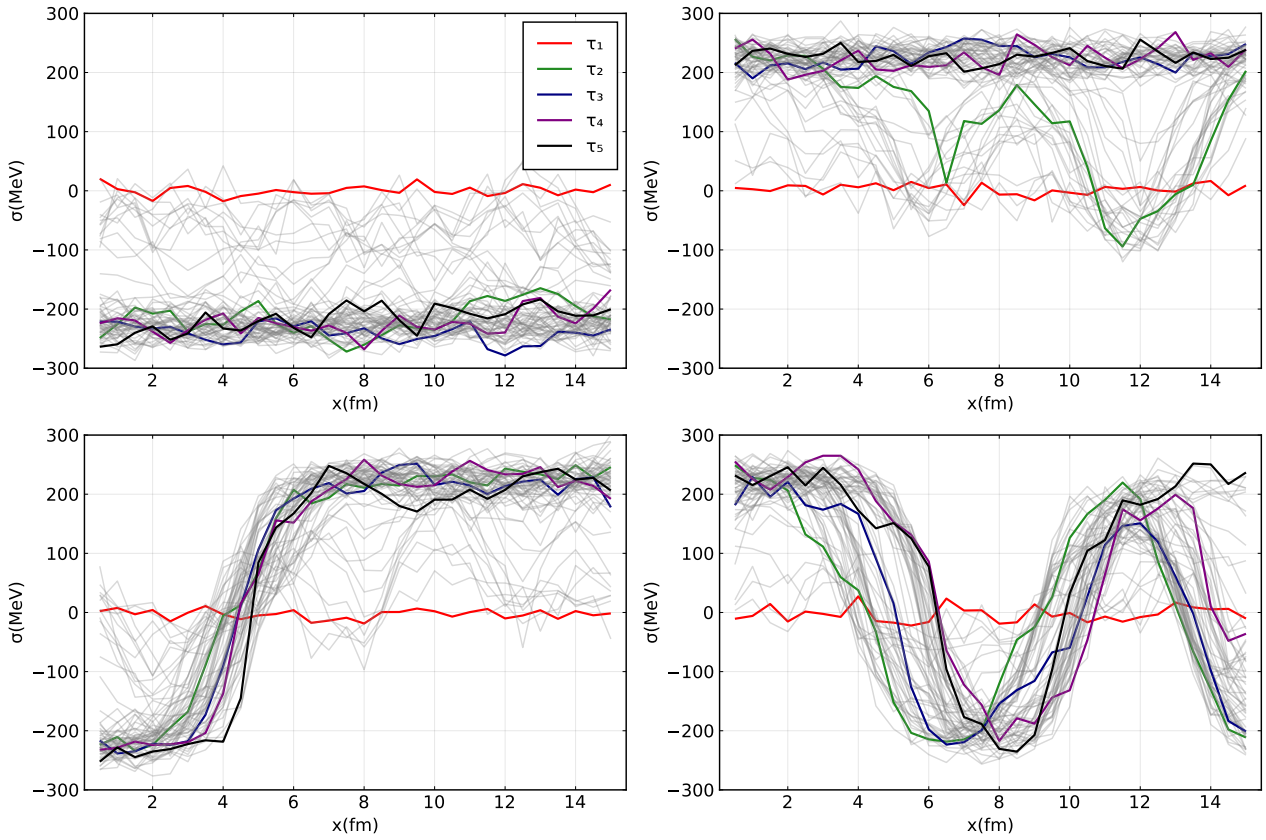


Figure 2. Snapshots of archetypic evolutions of the condensate in 1 + 1 dimensions, including fluctuations. In the upper left and upper right, we see the system finds the homogeneous ground state and settles there quickly. In the other evolutions, the system adopts an inhomogeneous phase before it eventually decays into the homogeneous minimum.

The patterns are *all* of the RKC type. Note that in Figure 2, in the lower left plot, the system quickly finds a hyperbolic tangent shape and stays within that shape. This is a very common evolution. More than one third of our simulations show this behavior. As always, though, they eventually decay down to a homogeneous phase. However, it is interesting to see that even in a model where an RKC is not found in the phase diagram, it does show up in the evolution. The lower right plot is a two-kink structure, which is also found in other lower-dimensional models [50].

4.2. 2 + 1 Dimensions

In 2 + 1 dimensions, one can still find similar behavior to 1 + 1; that is, we can find a long-lasting pattern forming. Each line of plots in Figure 3 shows different event evolutions. The red surface plots (first column) are the initial conditions, and the green and blue (middle column and right column) surfaces show subsequent time slices. It is noteworthy, however, that by opening up another spatial direction, patterned phases do not become less common. For instance, in the 1 + 1 systems, roughly one third of all evolutions quickly converge to the homogeneous minimum and stay there indefinitely. The rest all settles on an inhomogeneous phase temporarily. The proportion is roughly the same for 2 + 1 dimensions.

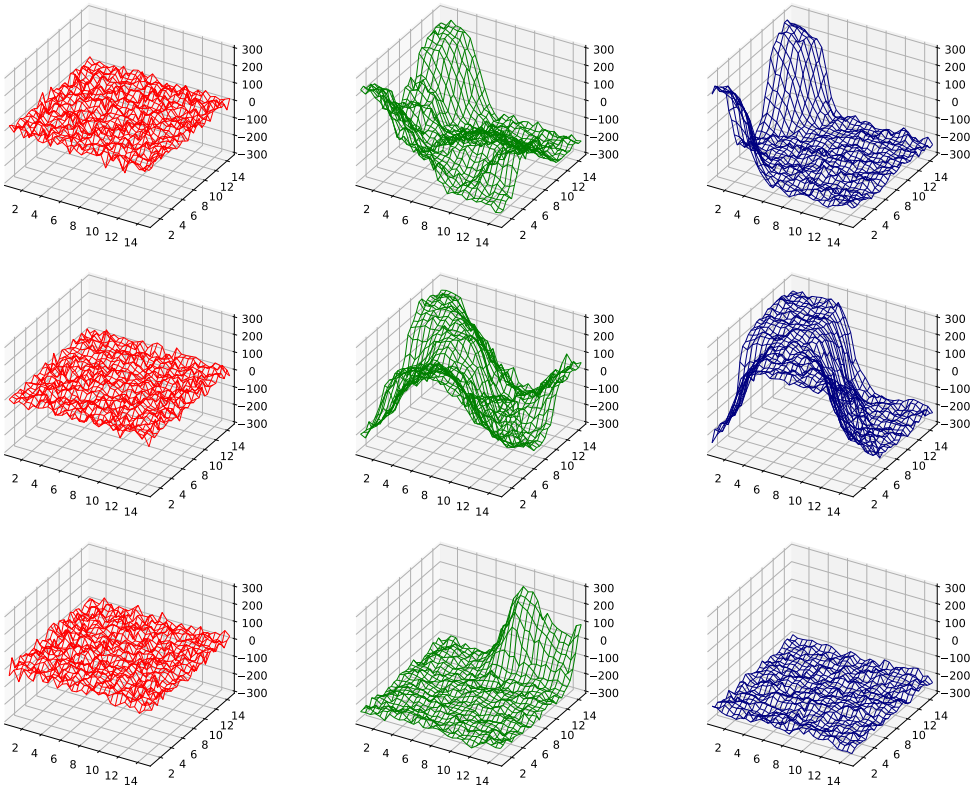


Figure 3. Archetypic evolutions in 2 + 1 dimensions. Red, green and blue correspond, respectively, to the initial state and two progressively advanced intermediary stages.

Most interestingly, the more time-persistent inhomogeneous phases in 2 + 1 dimensions are one-dimensional inhomogeneous patterns extruded linearly in a direction orthogonal to the pattern formation, that is:

$$\sigma(x_1, x_2, \tau) \propto M_{1D}(\lambda_1 x_1 + \lambda_2 x_2), \tag{15}$$

where M_{1D} corresponds to Equation (1). In Figure 3, this corresponds to the last time slice (blue surface plot) of the second evolution. This is not surprising; many previous works

have used this as an Ansatz [10,13,51], and in fact, Ref. [15] verifies explicitly that the 1D modulations are preferred over the 2D modulations. Nevertheless, although not surprising, no past work has looked into how long these disfavored phases live before they decay to the homogeneous favored ones. It is impressive to observe that intricate two-dimensional modulating patterns are consistently disfavored, even transiently, in 2 + 1 dimensions.

4.3. 3 + 1 Dimensions

In three dimensions, which naturally is the most interesting scenario, the computational costs become truly significant, and an extensive statistical analysis is costly. However, here as well, one can find metastable inhomogeneous phases, although it seems to be the case that they are less frequently formed. Figure 4 shows the time evolution of one event: the initial stage, which is again fluctuations around zero, and two subsequent time slices.

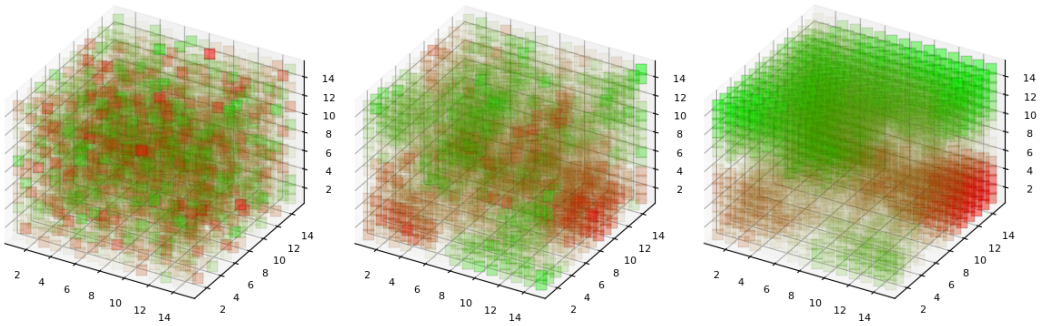


Figure 4. One evolution in 3 + 1 dimensions. Red and green here symbolize the opposite degenerate minima of the homogeneous potential.

5. Discussion and Conclusions

This event-by-event analysis shows that it is possible to form spatially nontrivial condensates as the system cools down from the restored phase back to the broken phase. A complete statistical analysis, which we postpone to a future publication, must involve averages over multiple evolutions, showing the fraction of long-lived patterned configurations over the homogeneous ones, as a function of temperature, chemical potential, and the system size. Furthermore, the exact time scales are important, of course, and we discuss them shortly. However, the findings of Refs. [29,30] indubitably persist in the presence of thermal fluctuations, modeled by the ξ field, and in higher dimensional spaces. If inhomogeneous phases do turn out to be disfavored in equilibrium, they might still play a role in the evolution of out-of-equilibrium quark matter. This is relevant for lower energy heavy-ion collisions, such as the ones expected to take place at the Facility for Antiproton and Ion Research (FAIR) . Moreover, it might also be relevant for neutron star merger events. As the stars merge, the dense and cold matter in their nuclei heat up and are pushed out of equilibrium. If chiral symmetry is restored and then cooled down back towards the broken phase, these phases could be phenomenologically relevant.

An associated phenomenon to spatially modulated phases is the so-called moat regime [52,53]. In a moat regime, the mesonic dispersion relation becomes nonmonotonic, and a nonzero three-momentum becomes energetically favored. This is the case for inhomogeneous phases; however, some types of disordered phases also manifest a moat regime such as liquid crystals and the so-called quantum–pion liquid [23,54]. These might leave signatures in heavy-ion collisions [53,55,56]

In order to have a true estimate of the lifetime of these phases, one must calculate the dissipation coefficient η. This, in principle, can be performed using the influence functional formalism. However, according to Refs. [31,32], a lower estimate of the σ dissipation parameter for $\mu = 0$ is roughly $\eta_\sigma \approx 3 - 4\ \mathrm{fm}^{-1}$. This value increases for larger

temperatures; so, one can take this as a lower bound. Using this value, the last time slice shown in Figure 2, labeled as τ_5, would correspond to 3.5–4.8 fm/c. The question, however, is how long it takes for this phase to decay entirely to the homogeneous minimum. For most of our simulations, in 1 + 1 dimensions, the events with the least long-lived patterns take timescales of order 100 fm/c to decay; some can last up to 10^4 fm/c. Since the simulations become more expensive for 2 + 1 and 3 + 1 dimensions, we did not move as far. The blue surface plots shown in Figure 3, assuming $\eta_\sigma = 4$ fm^{-1}, are at $t = 7.2$ fm/c, and they are expected to live for far longer times.

Author Contributions: Conceptualization, T.F.M. and G.K.; Methodology, T.F.M. and G.K.; Software, T.F.M.; Writing — review & editing, T.F.M. and G.K.; Supervision, G.K.; Funding acquisition, G.K. All authors have read and agreed to the published version of the manuscript.

Funding: This work was partially financed by Fundação de Amparo à Pesquisa do Estado de São Paulo (FAPESP), grant no. 2024/13426-0 (TFM) and 2018/25225-9 (GK), and Conselho Nacional de Desenvolvimento Científico e Tecnológico (CNPq), grant no. 309262/2019-4.

Data Availability Statement: Data will be made available upon request.

Conflicts of Interest: The authors declare no conflicts of interest. The funders had no role in the design of the study; in the collection, analysis or interpretation of data; in the writing of the manuscript, or in the decision to publish the results.

References

1. Overhauser, A.W. Structure of Nuclear Matter. *Phys. Rev. Lett.* **1960**, *4*, 415–418. [CrossRef]
2. Motta, T.F.; Bernhardt, J.; Buballa, M.; Fischer, C.S. Inhomogenuous instabilities at large chemical potential in a rainbow-ladder QCD model. *arXiv* **2024**, arXiv:2406.00205. [CrossRef]
3. Motta, T.F.; Bernhardt, J.; Buballa, M.; Fischer, C.S. Toward a stability analysis of inhomogeneous phases in QCD. *Phys. Rev. D* **2023**, *108*, 114019. [CrossRef]
4. Motta, T.F.; Buballa, M.; Fischer, C.S. New Tool to Detect Inhomogeneous Chiral Symmetry Breaking. *arXiv* **2024**, arXiv:2411.02285.
5. Thies, M. From relativistic quantum fields to condensed matter and back again: Updating the Gross-Neveu phase diagram. *J. Phys. A* **2006**, *39*, 12707–12734. [CrossRef]
6. Koenigstein, A.; Pannullo, L.; Rechenberger, S.; Steil, M.J.; Winstel, M. Detecting inhomogeneous chiral condensation from the bosonic two-point function in the (1 + 1)-dimensional Gross–Neveu model in the mean-field approximation. *J. Phys. A* **2022**, *55*, 375402. [CrossRef]
7. Ciccone, R.; Pietro, L.D.; Serone, M. Inhomogeneous Phase of the Chiral Gross-Neveu Model. *Phys. Rev. Lett.* **2022**, *129*, 071603. [CrossRef]
8. Koenigstein, A.; Winstel, M. Revisiting the spatially inhomogeneous condensates in the $(1+1)$-dimensional chiral Gross–Neveu model via the bosonic two-point function in the infinite-N limit. *J. Phys. A* **2024**, *57*, 335401. [CrossRef]
9. Buballa, M.; Carignano, S. Inhomogeneous chiral phases away from the chiral limit. *Phys. Lett. B* **2019**, *791*, 361–366. [CrossRef]
10. Buballa, M.; Carignano, S. Inhomogeneous chiral condensates. *Prog. Part. Nucl. Phys.* **2015**, *81*, 39–96. [CrossRef]
11. Buballa, M.; Carignano, S.; Kurth, L. Inhomogeneous phases in the quark-meson model with explicit chiral-symmetry breaking. *Eur. Phys. J. Spec. Top.* **2020**, *229*, 3371–3385. [CrossRef]
12. Tripolt, R.A.; Schaefer, B.J.; von Smekal, L.; Wambach, J. Low-temperature behavior of the quark-meson model. *Phys. Rev. D* **2018**, *97*, 034022. [CrossRef]
13. Nickel, D. Inhomogeneous phases in the Nambu-Jona-Lasino and quark-meson model. *Phys. Rev. D* **2009**, *80*, 074025. [CrossRef]
14. Thies, M. Nonperturbative phase boundaries in the Gross-Neveu model from a stability analysis. *Phys. Rev. D* **2024**, *110*, 096012. [CrossRef]
15. Pannullo, L.; Wagner, M.; Winstel, M. Inhomogeneous Phases in the Chirally Imbalanced 2 + 1-Dimensional Gross-Neveu Model and Their Absence in the Continuum Limit. *Symmetry* **2022**, *14*, 265. [CrossRef]
16. Winstel, M.; Pannullo, L. Stability of homogeneous chiral phases against inhomogeneous perturbations in 2 + 1 dimensions. *PoS* **2023**, *LATTICE2022*, 195. [CrossRef]
17. Pannullo, L. Inhomogeneous condensation in the Gross-Neveu model in noninteger spatial dimensions $1 \leq \mathrm{d} < 3$. *Phys. Rev. D* **2023**, *108*, 036022. [CrossRef]

18. Koenigstein, A.; Pannullo, L. Inhomogeneous condensation in the Gross-Neveu model in noninteger spatial dimensions $1 \leq d < 3$. II. Nonzero temperature and chemical potential. *arXiv* **2023**, arXiv:2312.04904.
19. Buballa, M.; Kurth, L.; Wagner, M.; Winstel, M. Regulator dependence of inhomogeneous phases in the (2 + 1)-dimensional Gross-Neveu model. *Phys. Rev. D* **2021**, *103*, 034503. [CrossRef]
20. Pannullo, L.; Wagner, M.; Winstel, M. Inhomogeneous phases in the 3 + 1-dimensional Nambu-Jona-Lasinio model and their dependence on the regularization scheme. *PoS* **2023**, *LATTICE2022*, 156. [CrossRef]
21. Pannullo, L.; Wagner, M.; Winstel, M. Regularization effects in the Nambu-Jona-Lasinio model: Strong scheme dependence of inhomogeneous phases and persistence of the moat regime. *arXiv* **2024**, arXiv:2406.11312. [CrossRef]
22. Pannullo, L. Inhomogeneous Phases and the Moat Regime in Nambu-Jona-Lasinio-Type Models. Ph.D. Thesis, Frankfurt Uiversity, Frankfurt am Main, Germany, 2024. [CrossRef]
23. Pisarski, R.D.; Tsvelik, A.M.; Valgushev, S. How transverse thermal fluctuations disorder a condensate of chiral spirals into a quantum spin liquid. *Phys. Rev. D* **2020**, *102*, 016015. [CrossRef]
24. Pisarski, R.D.; Skokov, V.V.; Tsvelik, A.M. Fluctuations in cool quark matter and the phase diagram of Quantum Chromodynamics. *Phys. Rev. D* **2019**, *99*, 074025. [CrossRef]
25. Goldenfeld, N. *Lectures on Phase Transitions and the Renormalization Group*; Perseus Books: Reading, UK, 1992.
26. Onuki, A. *Phase Transition Dynamics*; Cambridge University Press: Cambridge, UK, 2002.
27. Carlomagno, J.P.; Gomez Dumm, D.; Scoccola, N.N. Generalized Ginzburg-Landau approach to inhomogeneous phases in nonlocal chiral quark models. *Phys. Lett. B* **2015**, *745*, 1–4. [CrossRef]
28. Carlomagno, J.P.; Gómez Dumm, D.; Scoccola, N.N. Inhomogeneous phases in nonlocal chiral quark models. *Phys. Rev. D* **2015**, *92*, 056007. [CrossRef]
29. Carlomagno, J.P.; Krein, G. Time-dependent Ginzburg-Landau approach to the dynamics of inhomogeneous chiral condensates in a nonlocal Nambu–Jona-Lasinio model. *Phys. Rev. D* **2018**, *98*, 014015. [CrossRef]
30. Carlomagno, J.P.; Krein, G.; Kroff, D.; Peixoto, T. Dynamics of inhomogeneous chiral condensates. *EPJ Web Conf.* **2018**, *172*, 03005. [CrossRef]
31. Rischke, D.H. Forming disoriented chiral condensates through fluctuations. *Phys. Rev. C* **1998**, *58*, 2331–2357. [CrossRef]
32. Nahrgang, M.; Leupold, S.; Herold, C.; Bleicher, M. Nonequilibrium chiral fluid dynamics including dissipation and noise. *Phys. Rev. C* **2011**, *84*, 024912. [CrossRef]
33. Krein, G.; Miller, C. Nonequilibrium Dynamics of the Chiral Quark Condensate under a Strong Magnetic Field. *Symmetry* **2021**, *13*, 551. [CrossRef]
34. Ferrer, E.J.; de la Incera, V. Magnetic Dual Chiral Density Wave: A Candidate Quark Matter Phase for the Interior of Neutron Stars. *Universe* **2021**, *7*, 458. [CrossRef]
35. Nakano, E.; Tatsumi, T. Chiral symmetry and density wave in quark matter. *Phys. Rev. D* **2005**, *71*, 114006. [CrossRef]
36. Müller, D.; Buballa, M.; Wambach, J. Dyson-Schwinger study of chiral density waves in QCD. *Phys. Lett. B* **2013**, *727*, 240–243. [CrossRef]
37. Kojo, T.; Hidaka, Y.; McLerran, L.; Pisarski, R.D. Quarkyonic Chiral Spirals. *Nucl. Phys. A* **2009**, *843*, 37–58. [CrossRef]
38. Nishiyama, K.; Karasawa, S.; Tatsumi, T. Hybrid chiral condensate in the external magnetic field. *Phys. Rev. D* **2015**, *92*, 036008. [CrossRef]
39. Başar, G.; Dunne, G.V. Twisted kink crystal in the chiral Gross-Neveu model. *Physical Review D* **2008**, *78*, 065022. [CrossRef]
40. Basar, G.; Dunne, G.V.; Thies, M. Inhomogeneous Condensates in the Thermodynamics of the Chiral NJL(2) model. *Phys. Rev. D* **2009**, *79*, 105012. [CrossRef]
41. Colangelo, G.; Durr, S. The Pion mass in finite volume. *Eur. Phys. J. C* **2004**, *33*, 543–553. [CrossRef]
42. FLAG Working Group; Aoki, S.; Bernard, C.; Blum, T.; Colangelo, G.; Della Morte, M.; Dürr, S.; El-Khadra, A.X.; Fukaya, H.; Horsley, R.; et al. Review of Lattice Results Concerning Low-Energy Particle Physics. *Eur. Phys. J. C* **2014**, *74*, 2890. [CrossRef]
43. Bowler, R.D.; Birse, M.C. A Nonlocal, covariant generalization of the NJL model. *Nucl. Phys. A* **1995**, *582*, 655–664. [CrossRef]
44. Diakonov, D.; Petrov, V.Y. Meson Current Correlation Functions in Instanton Vacuum. *Sov. Phys. JETP* **1985**, *62*, 431–437.
45. Diakonov, D.; Petrov, V.Y.; Pobylitsa, P.V. A Chiral Theory of Nucleons. *Nucl. Phys. B* **1988**, *306*, 809. [CrossRef]
46. Calzetta, E.A.; Hu, B.L.B. *Nonequilibrium Quantum Field Theory*; Cambridge Monographs on Mathematical Physics; Cambridge University Press: Cambridge, UK, 2008. [CrossRef]
47. Blaschke, D.; Aichelin, J.; Bratkovskaya, E.; Friese, V.; Gazdzicki, M.; Randrup, J.; Rogachevsky, O.; Teryaev, O.; Toneev, V. Topical issue on Exploring Strongly Interacting Matter at High Densities—NICA White Paper. *Eur. Phys. J. A* **2016**, *52*, 267. [CrossRef]
48. Agarwal, K. The compressed baryonic matter (CBM) experiment at FAIR—physics, status and prospects. *Phys. Scr.* **2023**, *98*, 034006. [CrossRef]
49. Aoki, K.; Fujioka, H.; Gogami, T.; Hidaka, Y.; Hiyama, E.; Honda, R.; Hosaka, A.; Ichikawa, Y.; Ieiri, M.; Isaka, M.; et al. Extension of the J-PARC Hadron Experimental Facility: Third White Paper. *arXiv* **2021**, arXiv:2110.04462.

50. Carignano, S.; Nickel, D.; Buballa, M. Influence of vector interaction and Polyakov loop dynamics on inhomogeneous chiral symmetry breaking phases. *Phys. Rev. D* **2010**, *82*, 054009. [CrossRef]
51. Nickel, D. How many phases meet at the chiral critical point? *Phys. Rev. Lett.* **2009**, *103*, 072301. [CrossRef]
52. Pisarski, R.D.; Rennecke, F. Signatures of Moat Regimes in Heavy-Ion Collisions. *Phys. Rev. Lett.* **2021**, *127*, 152302. [CrossRef]
53. Rennecke, F.; Pisarski, R.D. Moat Regimes in QCD and their Signatures in Heavy-Ion Collisions. *PoS* **2022**, *CPOD2021*, 016. [CrossRef]
54. Winstel, M.; Valgushev, S. Lattice study of disordering of inhomogeneous condensates and the Quantum Pion Liquid in effective $O(N)$ model. In Proceedings of the Excited QCD 2024 Workshop, Benasque, Spain, 14–20 January 2024.
55. Nussinov, Z.; Ogilvie, M.C.; Pannullo, L.; Pisarski, R.D.; Rennecke, F.; Schindler, S.T.; Winstel, M. Dilepton production from moaton quasiparticles. *arXiv* **2024**, arXiv:2410.22418.
56. Rennecke, F.; Pisarski, R.D.; Rischke, D.H. Particle interferometry in a moat regime. *Phys. Rev. D* **2023**, *107*, 116011. [CrossRef]

Disclaimer/Publisher's Note: The statements, opinions and data contained in all publications are solely those of the individual author(s) and contributor(s) and not of MDPI and/or the editor(s). MDPI and/or the editor(s) disclaim responsibility for any injury to people or property resulting from any ideas, methods, instructions or products referred to in the content.